

Real-time detection of laser-induced transient gratings and surface acoustic wave pulses with a Michelson interferometer

Yao-chun Shen^{a)} and Peter Hess^{b)}

Institute of Physical Chemistry, University of Heidelberg, Im Neuenheimer Feld 253, D-69120 Heidelberg, Germany

(Received 27 May 1997; accepted for publication 11 August 1997)

Laser-induced transient gratings (LITGs) at surfaces of absorbing materials were utilized to generate narrowband surface acoustic waves (SAWs). In these experiments, SAWs were excited thermoelastically by two crossed picosecond laser pulses and detected with an actively stabilized Michelson interferometer by measuring transient surface displacements in the sub-angstrom range in real time. In addition, coherent broadband SAW pulses with frequencies up to 350 MHz were excited by sharply focusing the laser beam with a cylindrical lens system onto the sample surface. The LITG experiments provide an extension of the frequency range achieved with the broadband SAW pulse technique. From the measurements of the dispersive SAW phase velocity for a 650 nm aluminum film on fused silica in the frequency range 10 MHz–1 GHz the density and elastic constants were determined by fitting the experimental data to the exact solution of the wave equations taking into account the boundary conditions. © 1997 American Institute of Physics. [S0021-8979(97)05522-9]

I. INTRODUCTION

The laser-induced transient grating (LITG) technique has been successfully applied to investigate material properties in a wide range of systems.^{1–3} In LITG experiments, two temporally coincident laser pulses (pump pulses) are crossed at the sample surface. Absorption of crossed laser pulses in a sample gives rise to spatially periodic heating and thermal expansion, which launches counterpropagating acoustic waves. The acoustic oscillations and their decay, and finally the thermal diffusion, are usually monitored through the measurement of the time-dependent diffraction of a third probe beam, and provide information about the thermal and elastic properties of thin-film and bulk materials.^{4–7} In previous experiments, the time dependence of the response was obtained by repeating the excitation-probe pulse sequence with different delays of the probe relative to the pump. This leads to long data collection times and in some cases to cumulative sample heating and even damage. Recently, real-time measurements have been achieved by using a cw laser or “quasi-cw” laser pulse as the probe beam.^{8–10}

In all these experiments, gratings were detected via probe-beam diffraction. Matthias and co-workers¹¹ reported on the detection of transient thermal gratings via the angular deflection of a strongly focused probe beam. This allows the separation of surface displacement contributions from the modulation of the refractive index due to temperature and strain variation.^{12,13} However, no surface acoustic wave (SAW) oscillations could be monitored in their experiments due to the relatively poor time resolution of about 50 ns.¹¹ In this article, we will report on the detection of LITGs with an actively stabilized Michelson interferometer. Using an interferometer to measure the SAW oscillations on the sample

surface allows real-time data acquisition and an exact determination of the transient surface displacement. At the same time the interferometer probe scheme provides the possibility of studying the propagation behavior (such as attenuation) of the SAW oscillations generated from LITGs. Moreover, the LITG experiments can be combined with broadband SAW spectroscopy, generating short SAW pulses by confining the laser excitation in space and time.¹⁴ This technique has been widely applied to determine the mechanical and elastic properties of various films.^{15,16}

II. EXPERIMENT

In all experiments a frequency-tripled Nd:YAG laser with a wavelength of 355 nm and a pulse duration of 180 ps full width half maximum (FWHM) was used as the pump laser to excite SAWs. The sample investigated was an aluminum film, which was evaporated onto a fused silica substrate using a quartz-crystal microbalance as thickness monitor. The thickness of the aluminum film was determined more accurately afterwards by a stylus-type profilometer to be 650 nm.

The laser generation and detection of narrowband SAW trains and broadband SAW pulses is schematically illustrated in Figs. 1 and 2, respectively. As can be seen in Fig. 1, narrowband SAWs are excited thermoelastically via the LITG method. Two ps laser pulses of wavelength λ are crossed at the sample surface, resulting in an optical interference fringe pattern, characterized by the grating period Λ [$\Lambda = \lambda/2 \sin(\theta/2)$, where θ is the angle between the excitation beams]. Optical absorption leads to rapid heating and thermal expansion, resulting in the generation of counterpropagating acoustic waves with wavelength Λ , as well as the formation of a steady-state thermal grating, which slowly decays via thermal diffusion.^{2,6} The excitation beams were focused by a cylindrical lens to an area of 3 mm length in the direction of SAW propagation (grating direction) and 0.5

^{a)}On leave from National Laboratory of Molecular and Biomolecular Electronics, Southeast University, Nanjing 210096, People's Republic of China.

^{b)}Corresponding author; Electronic mail: peter.hess@urz.uni-heidelberg.de

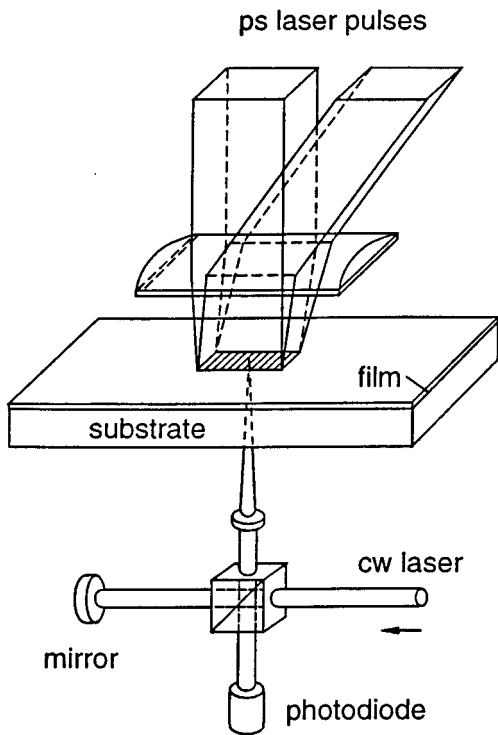


FIG. 1. Scheme of laser generation and detection of narrowband SAW trains. Two crossing ps laser pulses were focused with a cylindrical lens system onto the sample surface, forming a grating with an area of $3\text{ mm} \times 0.5\text{ mm}$ for narrowband SAW excitation via LITG.

mm width. This geometry produces more than 100 interference fringes, thus accurately fixing the wavelength and ensuring that the acoustic waves do not propagate too rapidly out of the excitation and probing region.¹⁷ Experiments were performed for grating periods ranging from 3.97 to $11.6\text{ }\mu\text{m}$ by changing the angle θ between the two excitation beams. The total energy incident on the sample surface was below 0.3 mJ for all LITG experiments. The dimensionless diffraction parameter $D = (8xv/\pi fb^2)$,¹⁸ where $b = 0.5\text{ mm}$ is the width of the grating, was small (about 0.17) even at the largest distance of $x = 1.5\text{ mm}$ and for the relatively low frequency of $f = 300\text{ MHz}$ with a phase velocity of about $v = 3370\text{ m/s}$. Thus diffraction effects can be neglected over the whole frequency range in the LITG experiments.

The laser-generated narrowband SAWs were monitored with a Michelson interferometer from the back side, where the metal-quartz interface acts as one of the mirrors and the detection system is actively stabilized.¹⁹ The probe beam was focused with a spherical lens system to a spot of about $1\text{ }\mu\text{m}$ diameter on the sample surface, at the center of the excitation region as indicated in Fig. 1. The detected signal was preamplified, stored, and averaged by a digitizing oscilloscope (Tektronix TDS 680B) with an analog bandwidth of 1 GHz and a sampling rate of 5 GS/s triggered by a fast photodiode. Usually the signal was averaged over 300 laser pulses in order to improve the signal-to-noise (S/N) ratio. The SAW wavelength was determined by the excitation geometry and the SAW frequency could be obtained by Fourier transformation of the SAW signal measured in the time do-

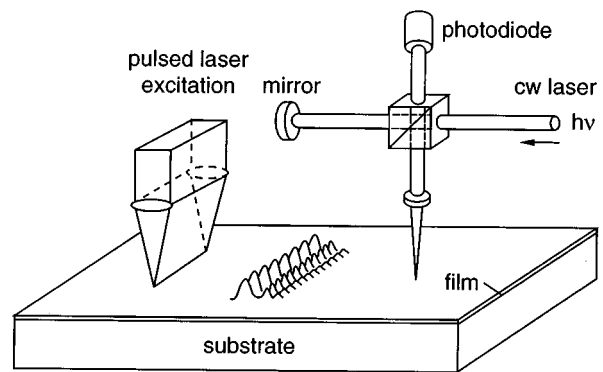


FIG. 2. Schematic representation of the pulsed laser generation and detection of broadband SAW pulses. The laser beam was sharply focused with a cylindrical lens system onto the sample surface, forming a narrow line source ($6\text{ }\mu\text{m} \times 10\text{ mm}$) for broadband SAW pulse excitation.

main. Therefore the SAW phase velocity could be calculated from these measurements.

To excite coherent broadband SAW pulses, the ps laser pulse was focused as sharply as possible through a cylindrical lens system onto the sample surface, forming a line source about 10 mm long and $6\text{ }\mu\text{m}$ wide (see Fig. 2). The pulse energy in the focus was about $60\text{ }\mu\text{J}$. The laser-generated short SAW pulse propagating along the surface was detected with the above-mentioned interferometer at two distances several millimeters to some centimeters away from the source. Fourier transformation of the SAW pulse measured in the time domain yields the frequency spectrum of the SAW pulse. From the SAW signals detected at two different distances the phase velocity dispersion and attenuation of the SAW pulse can be extracted as a function of frequency.¹⁴ To obtain a dispersion curve of high quality usually 300 acoustic pulses were averaged in the time domain to improve the S/N ratio.

III. RESULTS

A. Broadband SAW pulses

Figure 3(a) shows the laser-generated broadband SAW signal after propagation of about 17 mm away from the line source along an aluminum film deposited on fused silica. A number of oscillations can be observed in the signal shape, indicating that SAW dispersion appeared during propagation. The Fourier transformation of this signal shows a frequency spectrum reaching 350 MHz , although the setup was able to detect frequencies up to 1 GHz . The main limiting factors were the width of the line focus, which was about $6\text{ }\mu\text{m}$ in the present experiments and attenuation. Figure 3(b) shows the corresponding dispersion curve as well as the calculated best theoretical fit using the exact solution of the theory of SAW propagation in layered materials as described in Ref. 20. Normal dispersion, i.e., a decrease of the SAW phase velocity with frequency, was observed. This result is reasonable since aluminum is softer than fused silica.

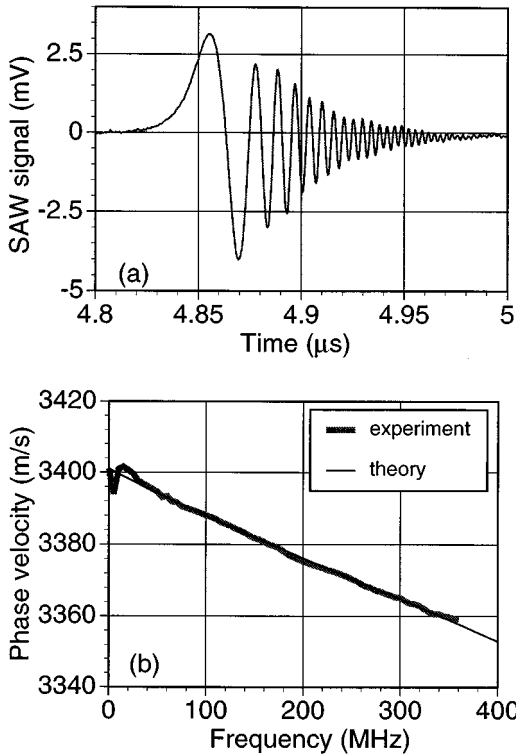


FIG. 3. SAW pulse shape after propagation of 17 mm (a) and normal dispersion curve for a 650 nm aluminum film deposited on a fused silica substrate (b). The ps laser pulse was focused to a line source on the aluminum surface to launch the plane SAW pulses.

B. Narrowband SAW from LITG

Figure 4(a) shows a typical LITG response for the 650 nm aluminum film on fused silica, for a grating period of $4.34 \mu\text{m}$. Excitation occurs at $t=0$, followed by fast oscillations and a slow overall decay. The slowly decaying component is due to heat diffusion, from which the thermal properties of the sample can be obtained.^{7,11} The oscillating component is due to the counterpropagation of SAWs. It becomes clear from Fig. 4(b) that these SAW oscillations have a narrow frequency range. The Fourier transformation of the high frequency oscillations, presented in the inset, yields a center frequency of 761 MHz. A SAW phase velocity of 3303 m/s was determined for these conditions. As stated before experiments were performed for acoustic wavelengths ranging from 3.97 to $11.6 \mu\text{m}$ covering the frequency range of 300–830 MHz. The measured dependence of the SAW phase velocity on frequency and the broadband results are presented in Fig. 5, along with the theoretical curve. As expected, the SAW phase velocity starts from the Rayleigh velocity of the fused silica substrate (Suprasil II, 3401 m/s) at the low frequency limit while approaching the Rayleigh velocity for aluminum (2940 m/s) at high frequencies.

The accuracy in the SAW velocity measured by LITG experiments is ultimately determined by the uncertainty in the frequency, which is given by the number of oscillations determined by the length of the excitation spot L . For $L = 3 \text{ mm}$ and a typical SAW velocity of $v = 3000 \text{ m/s}$, one finds an associated broadening of the frequency spectrum,

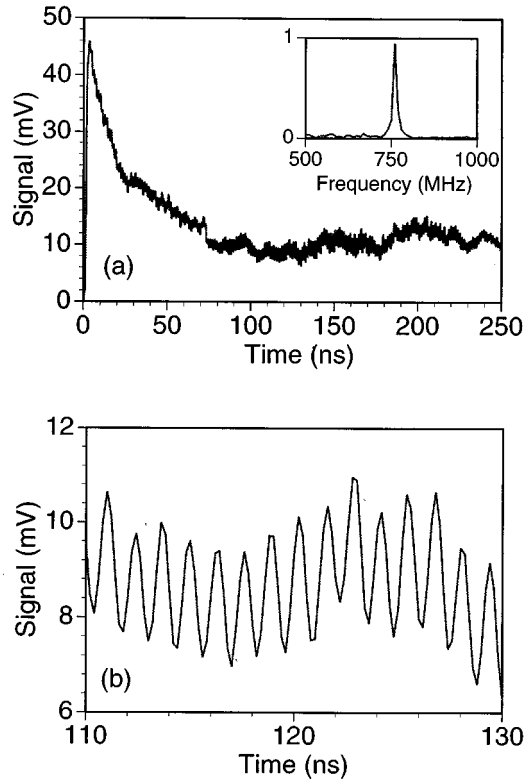


FIG. 4. (a) Typical LITG response of a 650 nm aluminum film on fused silica. The inset shows the Fourier transform of this signal. (b) The SAW signal between 110 and 130 ns is plotted for a better resolution.

$\delta\omega = 2v/L$, of about 2 MHz. At low frequencies, for example at 100 MHz, the accuracy of the LITG experiments is about 2%, while at high frequencies, for example at 1 GHz, LITG measurements can reach an accuracy of 0.2%. This is comparable to broadband SAW spectroscopy, where an accuracy of 0.1% in the determination of the SAW velocity can readily be achieved.¹⁴

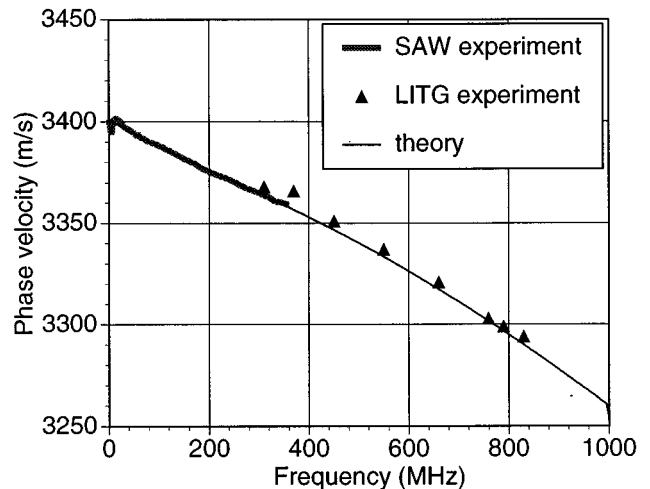


FIG. 5. Combined dispersion curves of broadband and narrowband experiments for a 650 nm aluminum film on fused silica.

C. Determination of film properties from the SAW dispersion

The dispersion curve was described theoretically by the exact solution of the wave equations taking into account the boundary conditions at the free film surface and the film-substrate interface.²⁰ Comparison of the calculated dispersion curve with experimental ones can be used to determine the elastic properties of an isotropic film. Let f_{\max} be the maximum frequency in the experimental signal spectrum with sufficiently high S/N ratio and k_{\max} be the corresponding wave number. Then the capability for the determination of film properties depends on the value achieved for the parameter $\gamma_{\max} = k_{\max}d$, where d is the film thickness. For $\gamma_{\max} < 0.1$, usually the determination of only one film parameter is possible. For larger values of γ_{\max} , two, three, or even four film parameters can be determined due to the increasing nonlinearity of the dispersion curve. In our experiments, γ_{\max} of value 0.36 was achieved for the broadband SAW spectroscopy and this value was increased to 1.03 by the LITG experiments. The film density ρ , Young's modulus E , and Poisson's ratio ν obtained from the best fit in Fig. 5 were 2.72 g/cm³, 73 GPa, and 0.34, respectively. This is consistent with literature values of bulk aluminum ($\rho = 2.70$ g/cm³, $E = 72.2$ GPa, and $\nu = 0.34$).²¹ Note that the extension of the frequency range by the LITG results improves the accuracy of the extracted film properties considerably.

IV. DISCUSSION

A. Laser detection of LITGs

We have shown in this article that LITGs can be detected efficiently with a Michelson interferometer by measuring the transient surface displacements quantitatively in real time. In contrast to traditional LITG experiments this allows the entire response to be measured with minimal signal averaging and even a single laser pulse can yield an adequate signal. The minimum detectable displacement δx for a Michelson interferometer is determined by $\delta x = (\lambda/4\pi) \times (2h\nu\Delta f/\eta W_0)^{1/2}$, where h is Planck's constant, η the quantum efficiency, Δf the bandwidth of the detection system, and λ , ν , and W_0 are the wavelength, the frequency, and the power of the probe beam, respectively. For a 40 mW probe laser with a wavelength of 532 nm and a detection bandwidth of 1 GHz we find $\delta x = 0.01$ nm. By using a stabilized cw Nd:YAG laser (532 nm, 120 mW) as the light source of the interferometer and a fast photodiode-amplifier system (Hamamatsu S4753 PIN photodiodes and Avantek INA-03184 amplifier) as detector, we were able to measure transient surface displacements in the sub-angstrom range with frequency components up to 1 GHz. We note that real-time detection has also been realized by using a fast photodetector to monitor the diffracted intensity of a cw or quasi-cw probe beam from the grating. The frequency range of this technique is limited only by the bandwidth of the photodetector and the oscilloscope, while the performance of the Michelson interferometer will also depend on the focus size of the probe beam.

In the probe-beam diffraction technique the spot size of the probe beam on the sample surface should be large enough to provide sufficient diffraction, while in the Michelson interferometer method the probe beam is sharply focused onto the sample surface. This makes it possible to measure the SAW oscillations resulting from a LITG not only in the LITG region but also outside it. In this case the slow thermal decay is not clouding the oscillatory signal but diffraction effects may occur at larger propagation distances. Thus the Michelson interferometer method provides the possibility of studying the propagation behavior of the SAW oscillations generated from LITGs.

B. Bandwidth of the SAW spectroscopy

Broadband SAW pulse experiments provide information on a wide frequency range of 1–2 orders of magnitude. In contrast to narrowband LITG experiments, where the SAW phase velocity can be determined only for one frequency in one experiment, the broadband SAW experiment has the ability to determine the whole dispersion curve of the SAW phase velocity in a frequency range from several megahertz to a few hundred megahertz in a single experiment. Therefore broadband SAW spectroscopy is a powerful method for the nondestructive evaluation of mechanical and elastic properties of thin-film materials. As demonstrated in Refs. 22 and 23 the simultaneous determination of up to four film parameters (Young's modulus, Poisson's ratio, film thickness, and density) is possible in a single experiment for films of about 1 μm thickness. For thinner films, however, only one or two film parameters can be determined by SAW spectroscopy in the frequency range achieved up to now since the dispersion curve is not nonlinear enough. The present frequency range of about 350 MHz is mainly limited by the focus width of the line source and attenuation of high frequencies.

A promising approach to extending the frequency range of SAW spectroscopy is provided by near-field optical techniques, where the Abbe diffraction limit in the optical regime can be overcome by using tapered optical fibers with a nanometer-sized aperture.²⁴ We have shown²⁵ that near-field optical fiber tips can indeed be applied for the laser generation of broadband SAW pulses. However, the SAW pulses launched by this technique are no longer plane waves, as studied here, because the optical fiber tip acts as a point source. This not only affects the attenuation, but in addition the anisotropic behavior of SAW pulses in anisotropic crystalline materials must be taken into account.²⁶

As we have shown here, the frequency range can be extended alternatively by using LITGs as an excitation source, where SAW oscillations with frequencies up to 3 GHz have been excited.^{6,7} By using a Michelson interferometer for detection, LITG experiments can be easily combined with broadband SAW spectroscopy by either focusing or defocusing the pump laser beams onto the sample surface. In the broadband SAW experiments the pump laser beam is sharply focused onto the sample surface, forming a narrow line source, while in the LITG experiments the two pump laser beams are defocused onto the sample surface, forming a larger grating area. The pulse experiment has the advantage of covering a wide frequency range and the grating experi-

ment possesses an inherently higher S/N ratio due to the very small bandwidth. The combination of LITG with broadband SAW spectroscopy allows the generation and detection of SAWs in an extremely wide frequency range and provides the possibility of determining both thermal and elastic film properties with high accuracy essentially in one experimental setup.

V. CONCLUSIONS

We conclude that narrowband SAW trains excited thermoelastically by two crossed ps laser pulses can be detected efficiently with a Michelson interferometer in and outside the source region by measuring transient surface displacements in the sub-angstrom range in real time. In contrast to traditional LITG experiments this allows the entire response to be measured with minimal signal averaging and even a single laser pulse may yield an adequate signal. LITG experiments can be easily combined with broadband SAW pulse spectroscopy to increase the information content (nonlinearity of the dispersion curve) for determining materials properties. This allows the laser generation and detection of SAWs in the widest frequency range realized up to now and provides the possibility of determining both thermal and elastic properties of thin films simultaneously in one experimental setup. We believe that this combined nondestructive diagnostic technique is of high potential for future scientific and technological applications.

ACKNOWLEDGMENTS

The authors thank R. Kuschnerit for his continuous help. Financial support of this work by the German-Israeli Foundation (GIF) for Scientific Research and Development is gratefully acknowledged. Y.C.S. thanks the Alexander von Humboldt Foundation for a fellowship. Additional support by the Fonds der Chemischen Industrie is gratefully acknowledged.

- ¹H. J. Eichler, P. Günter, and D. W. Pohl, *Laser-Induced Dynamic Gratings*, Springer Series in Optical Sciences (Springer, Berlin, Heidelberg, 1986), Vol. 50.
- ²K. A. Nelson, R. Casalegno, R. J. D. Miller, and M. D. Fayer, *J. Chem. Phys.* **77**, 1144 (1982).
- ³A. Harata, H. Nishimura, and T. Sawada, *Appl. Phys. Lett.* **57**, 132 (1990).
- ⁴C. D. Marshall, I. M. Fishman, and M. D. Fayer, *Phys. Rev. B* **43**, 2696 (1991).
- ⁵C. D. Marshall, A. Tokmakoff, I. M. Fishman, C. B. Eom, J. M. Phillips, and M. D. Fayer, *J. Appl. Phys.* **73**, 850 (1993).
- ⁶T. Sawada and A. Harata, *Appl. Phys. A: Solids Surf.* **61**, 263 (1995).
- ⁷Q. Shen, A. Harata, and T. Sawada, *J. Appl. Phys.* **77**, 1488 (1995).
- ⁸S. Kinoshita, Y. Shimada, W. Tsurumaki, M. Yamaguchi, and T. Yagi, *Rev. Sci. Instrum.* **64**, 3384 (1993).
- ⁹J. A. Rogers and K. A. Nelson, *J. Appl. Phys.* **75**, 1534 (1994).
- ¹⁰L. Dhar, J. A. Rogers, and K. A. Nelson, *J. Appl. Phys.* **77**, 4431 (1995).
- ¹¹O. W. Käding, H. Skurk, A. A. Maznev, and E. Matthias, *Appl. Phys. A: Solids Surf.* **61**, 253 (1995).
- ¹²A. R. Duggal, J. A. Rogers, and K. A. Nelson, *J. Appl. Phys.* **72**, 2823 (1992).
- ¹³A. Harata and T. Sawada, *Jpn. J. Appl. Phys., Part 1* **32**, 2188 (1993).
- ¹⁴A. Neubrand and P. Hess, *J. Appl. Phys.* **71**, 227 (1992).
- ¹⁵P. Hess, *Appl. Surf. Sci.* **106**, 429 (1996).
- ¹⁶D. Schneider and M. D. Tucker, *Thin Solid Films* **290**, 305 (1996).
- ¹⁷A. A. Maznev, K. A. Nelson, and T. Yagi, *Solid State Commun.* **100**, 807 (1996).
- ¹⁸A. A. Kolomenskii, A. M. Lomonosov, R. Kuschnerit, P. Hess, and V. E. Gusev, *Phys. Rev. Lett.* **79**, 1325 (1997).
- ¹⁹A. Neubrand, L. Konstantinov, and P. Hess, in *Physical Acoustics*, edited by O. Leyroy and M. A. Breazeale (Plenum, New York, 1991).
- ²⁰G. W. Farnell, in *Acoustic Surface Waves*, edited by A. A. Oliner, in *Topics in Applied Physics* (Springer, Berlin, 1978), Vol. 24, p. 42.
- ²¹*Handbook of Physics*, edited by S. Flügge (Springer, Berlin, 1973), Vol. VI, p. 1.
- ²²R. Kuschnerit, H. Fath, A. A. Kolomenskii, M. Szabadi, and P. Hess, *Appl. Phys. A: Solids Surf.* **61**, 269 (1995).
- ²³R. Kuschnerit and P. Hess, *Mater. Res. Soc. Symp. Proc.* **383**, 121 (1995).
- ²⁴E. Betzig and J. K. Trautman, *Science* **257**, 189 (1992).
- ²⁵Y. C. Shen and P. Hess, *Ultramicroscopy* (accepted).
- ²⁶A. A. Maznev, A. A. Kolomenskii, and P. Hess, *Phys. Rev. Lett.* **75**, 3332 (1995).